

KILN AERODYNAMICS VISUALISATION OF MERGING FLOW BY USAGE OF PIV AND CFD

I. A. Sofia LARSSON^{1*}, Elianne M. LINDMARK¹, T. Staffan LUNDSTRÖM¹, Daniel MARJAVAARA²
and Simon TÖYRÄ²

¹ Division of Fluid Mechanics, Luleå University of Technology, SE-971 87 Luleå, SWEDEN

² LKAB, Kiruna, SWEDEN

*Corresponding author, e-mail address: sofia.larsson@ltu.se

ABSTRACT

One way to upgrade iron ore is to process it into pellets. Such a process includes several stages involving complex fluid dynamics. In this work the focus is on the grate-kiln pelletizing process and especially on the rotary kiln, with the objective to get a deeper understanding of its aerodynamics. A down-scaled, simplified model of a full-scale kiln is created and both a numerical and an experimental analysis of the flow field are performed. Conclusions are that steady state simulations can be used to get an overview over the main features of the flow field. Precautions should though be taken when analysing the recirculation zone since the steady state simulations do not capture the transient, oscillating behaviour of the flow seen in the validation experiments, which affects the size of the recirculation zone.

INTRODUCTION

LKAB (Luossavaara-Kiirunavaara AB) is an international minerals group that produces iron ore products for the steel industry. LKAB's main product is iron ore pellets for production of hot metal in blast furnaces and direct reduction processes.

The crude ore from the mine often needs processing in order to get desirable properties and withstand transportation. This upgrade takes place in one or several ore processing plants, i.e. sorting, concentrating and pelletizing plants.

In the grate-kiln process, the pellets are first dried in the grate and then fired in the kiln. This gives them the hard surface they need to withstand long transports. The kiln is connected to an annular cooler which provides it with hot air, called secondary air. The mass flow of the secondary air is much higher than the primary air directly provided to the burner; hence the secondary air is likely to have a large influence of the flow field within the kiln. Therefore the geometry of the channels between the cooler and the kiln strongly affects the flow field in the kiln and hence the combustion. A sketch of a grate-kiln pelletizing plant is presented in Figure 1.

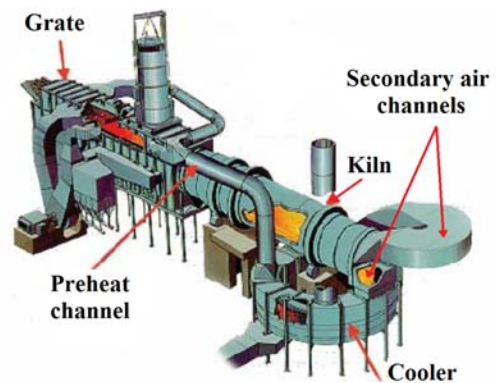


Figure 1: Grate-kiln pelletizing plant.

The pelletizing process is multifaceted involving a highly turbulent, high temperature flow in intricate geometries. This makes it a challenge to study. Little is known about the flow field in the different parts of the process thus motivating deeper studies of the process. In the present work the objective is to reveal flow features taking place in the kiln by doing simulations with Computational Fluid Dynamics (CFD) on a simplified model of a full-scale kiln, and validate different set-ups in the numerical model with physical experiments. There are at least two reasons to do this: to be able to decide if changes of the geometry up-stream the burner can alter the flow field in a way that improves the combustion and the pelletizing process, and to know how simple the set-up of the numerical simulation can be, still describing main features of the flow field. Later on a more realistic geometry may be studied with the validated simulations as a base. The commercial code ANSYS CFX 11.0 is used for the numerical simulations and they are validated by experiments on a physical model using Particle Image Velocimetry.

Kiln aerodynamics

Since fuel/air mixing largely controls the combustion process, the combustion air supply system and the resulting air flow patterns have a huge effect on the overall performance. The type of cooler, and its geometry, will define the secondary air flow regime and can result in severely distorted jet flows (and flames) as will also be shown in this study. Good flame stability is important for safe and efficient combustion. A stable flame has a constant point of ignition very close to the burner nozzle which is crucially determined by the recirculation zone that forms between the secondary flow inlet jets

(Mullinger and Jenkins, 2008). This zone is characterised by a rapid decay of the mean velocity compared to the surrounding flow field (Schneider et al., 2004) and it arises due to flow separation with the burner wall acting as a bluff body. Mullinger and Jenkins (2008) further explains the importance of this zone since it improves the flame stability as the reversed flow recirculates hot combustion products from downstream to mix with the incoming fuel stream and constantly ignites it. In this way the ignition point and flame are anchored to the burner nozzle which improves the combustion.

Only a small portion (10-30%) of the combustion air passes through the burner while the remaining part (secondary air) enters through the cooler and the kiln hood. Due to this fact the burner designer only have control of 10-30% of the air needed for combustion and hence more understanding of the secondary air flow regime can improve the combustion and reduce the emissions (Mullinger and Jenkins, 2008).

MODEL DESCRIPTION

Geometry

The model of the kiln is a simplified, down-scaled version of a real kiln and can be seen in Figure 2. The inlet channels are approximated as half circular channels. To achieve a fully developed velocity profile before entering the kiln, the length of the inlet channels are 4.0 m or 95 hydraulic diameters of the half circular channel. Dean and Bradshaw (1976) obtained fully developed flow in a rectangular duct after 93.6 hydraulic diameters for $Re = 1 \cdot 10^5$ (based on the height of the duct). To the authors knowledge similar results have not been presented for flow through half circular pipes.

The kiln is modelled as a straight horizontal cylinder without pellets while the real kiln has a smaller expansion in diameter and an inclination angle to the ground. The burner is excluded since only the cold flow field without combustion is of interest in this case.

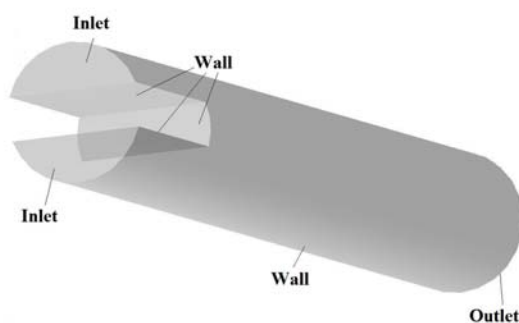


Figure 2: Geometry with boundaries (the full length of the inlet channels is not shown).

CFD set-up

The geometry is imported into ANSYS ICEM and a mesh consisting of hexahedral elements is created. An o-grid consisting of approximately 12.5 million nodes is designed in order to get a good mesh adaptation around the round edges. The y^+ values are in the range of 0.001 to 6 with an area averaged value of approximately 1.3, so the

boundary layer is not fully resolved everywhere in the geometry according to the requirements of low-Re wall formulations for an ω -based turbulence model (Ansys CFX-Solver Theory Guide, 2006). A mesh study was performed with $Re = 1 \cdot 10^4$ and with the efficiency factor as the dependent variable, defined as the ratio of mass averaged total pressure at the inlet to that at the outlet (Casey and Wintergerste, 2000). A conclusion from this study is that a mesh consisting of at least 3 million nodes is needed in order to achieve a grid independent solution. The reason for using 12.5 million nodes in the simulations is to resolve the boundary layer for higher Re. In order to maintain the mesh quality more nodes are placed in the flow direction to reduce the distance between the nodes in that direction and to keep the aspect ratio within an acceptable range.

Three dimensional, steady state, Reynolds averaged Navier-Stokes equations, closed by the Reynolds stress turbulence model BSL are solved for the turbulent flow field. A plug profile is used at the inlets and at the outlet an average static pressure is used with a relative pressure of zero Pa, averaged over the whole outlet. A second order discretisation scheme corresponding to Specified Blend Factor 1 is used. The convergence criterion is RMS residuals below 10^{-6} (Ansys CFX-Solver Theory Guide, 2006) and therefore double precision is used. No energy equation is used and the rotation of the real kiln is neglected in the model.

Experimental set-up

The experimental kiln has the same geometry as the virtual model, described in the previous section. To control the flow rate in the half circular pipes the flow is monitored with magnetic flow meters (Krohne Optiflux DN50) and the temperature in the set-up is monitored with a Pt100. The temperature of the water in the set-up is controlled to 20 ± 0.4 °C with a cooling system in the tank.

The PIV-system used is a commercially available system from LaVision GmbH. It consists of a Litron Nano L PIV laser, i.e. a double pulsed Nd:YAG with a maximum repetition rate of 100 Hz, and a LaVision FlowMaster Imager Pro CCD-camera with a spatial resolution of 1280 x 1024 pixels per frame. The laser is mounted on a traverse so that the laser sheet and camera can be repositioned up to 500 mm in the x-, y- and z-directions. The tracer particles used are hollow glass spheres with a diameter of 6 μm from LaVision GmbH.

PIV measurements are performed with a frequency of 80 Hz during 6 seconds which implies that for each measurement 480 frames are produced. In order to be able to compare the measurements to results from steady state simulations the 480 frames are time-averaged.

Measurements are taken in four different positions in the flow direction from the half circular pipes and downstream within the kiln. At each position measurements are performed on three planes directed along the flow, one in the middle and two on the sides. The order in which the positions are measured is randomized. In the post processing of the PIV measurements first a 64 x 64 pixels interrogation area is

used and then a 32 x 32 pixels, both with an overlap of 50%.

Numerical and experimental settings

The flow in the real kiln has a Reynolds number of approximately $8 \cdot 10^5$ based on the diameter of the kiln. In the experiment a Reynolds number of $5 \cdot 10^4$ and $1 \cdot 10^5$ is used, which corresponds to a mass flow of 3.95 kg/s and 7.9 kg/s respectively in the model kiln. The magnetic flow meters control the flow to an accuracy of 0.1% in the experiments. The fluid used in the model is water, allowing the smaller scale of the model kiln. Three distributions between the inlet channels are used, namely 50/50, 60/40 and 70/30 in order to detect how the distribution of mass flow affects the flow field in general and the recirculation zone in particular.

Most of the PIV measurements are presented as velocity plots in the centre of the channels with reference to their depths and where the fluid from the two inlet channels enters into the kiln. This is exemplified in Figure 4 showing 80 mm of the inlet channels to the left and 300 mm of the kiln (half of the total length) to the right. The laser can not illuminate the entire measuring section at one time so it has to be moved with the traverse to cover the area of interest. Hence several frames are linked together after each other to create a complete picture. Non continuous plots in the figures are due to; difficulties with overlapping the different frames into one picture, bad laser illumination at the borders of the measuring areas and joints in the geometry, especially where the inlet channels are connected to the kiln. Getting perfect optical availability at such a joint is rather tricky.

RESULTS

To start with, a visual comparison of the flow field in two different planes with equal off-set from the main axis of the kiln is performed to control that the flow field is axis-symmetric. As can be seen in Figure 3, there is no noticeable difference between the two planes, thus indicating that the flow field is axis-symmetric.

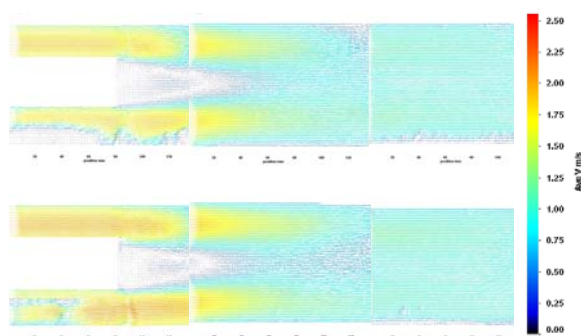


Figure 3: Equal flow distribution between the inlet channels in two different planes of the channel. The vectors denote time-averaged velocities over 6 seconds.

In order to derive the importance of applying the correct full-scale Re in the model, a comparison of the flow field for $Re = 5 \cdot 10^4$ and $1 \cdot 10^5$ is performed for the 50/50 distribution between the two inlet channels. The result shows that the flow field does not differ much between the two Res, disregarding the obvious velocity differences, see Figure 4. This indicates that an exact agreement of Re is not important as long as the Re used is within the fully

turbulent range, agreeing with the results reported by Yin et al. (2007). Hence, when measuring the 70/30 distribution Re is set to $5 \cdot 10^4$ for the simple reason that the pump used in the experiments can not manage that distribution at $Re = 1 \cdot 10^5$.

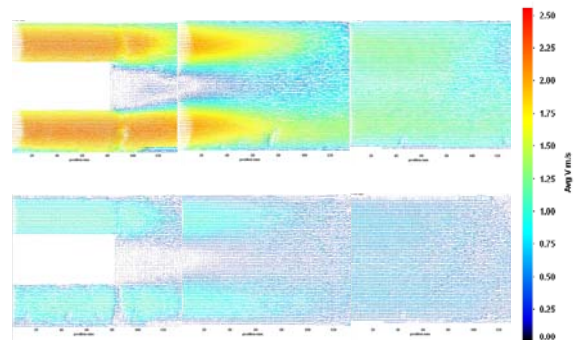


Figure 4: Equal flow distribution between the inlet channels (time-averaging over 6 seconds) for $Re = 1 \cdot 10^5$ at the top and $5 \cdot 10^4$ at the bottom.

The effect of gravity on the flow field is also investigated with usage of the PIV measurements by first pumping 60% of the mass flow through the top inlet channel and then in the lower one. The flow fields for the two cases are practically mirror images of each other, see Figure 5. This indicates that the gravity does not need to be taken into consideration when performing the simulations.

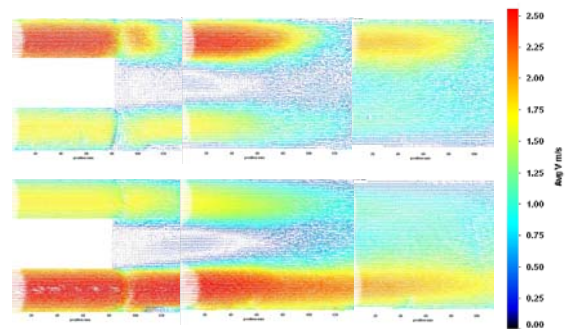


Figure 5: Different distributions in the inlet channels (time-averaging over 6 seconds), 60/40 at the top and 40/60 at the bottom.

Comparisons between simulation results based on a stationary set-up and time-averaged PIV measurements can be seen in Figures 6-8 for the distributions 50/50, 60/40 and 70/30.

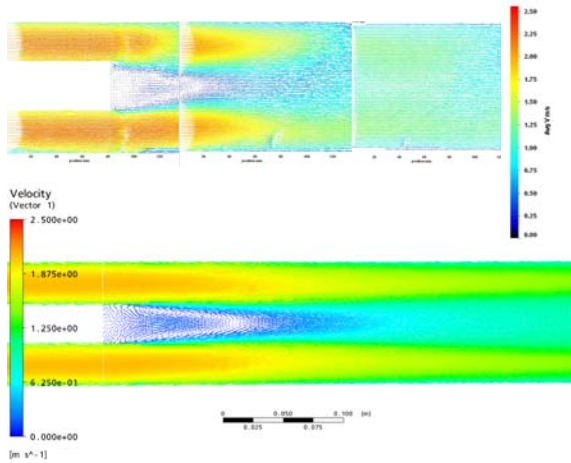


Figure 6: Equal distribution in the inlet channels. Velocity vectors, PIV results (time-averaging over 6 seconds) at the top, simulation results down below.

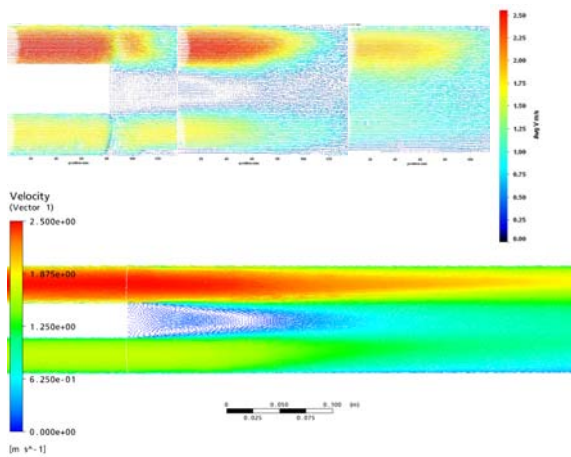


Figure 7: 60/40 distribution in the channels. Velocity vectors, PIV results (time-averaging over 6 seconds) at the top, simulation results down below.

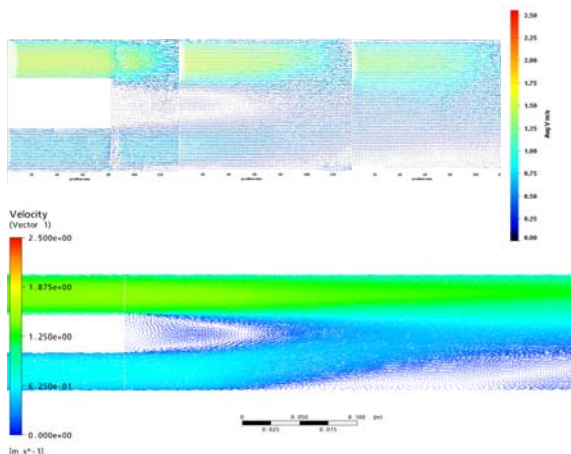


Figure 8: 70/30 distribution in the channels. Velocity vectors, PIV results (time-averaging of 6 seconds) at the top, simulation results down below.

The feature that all three cases have in common is that the inlet jets travel much further into the kiln in the simulations than in the experiments. This can be explained by the transient behaviour of the flow field in the experiments. The flow is oscillating which improves the mixing of the two inlet jets and lessens their strength. This behaviour is not captured with steady state simulations, allowing the jets to reach farther down-stream the inlets. The largest amplitudes of the oscillations in the experiments are found when the mass flow distribution between the inlet channels is equal. When one of the inlet jets starts to become dominant the other jet is pulled towards the dominant one and the flow field is stabilised, agreeing with the results reported by Bunderson and Smith (2005). This can clearly be seen in the experimental case with the 70/30 distribution.

One measure of particular interest is the length of the recirculation zone (RZ) that takes shape in between the two inlet jets, in front of the wall where the burner is located in the real kiln. The recirculation zone is important for the flame stability as outlined in the introduction. The length of this zone can be derived by usage of velocity contour plots where the transition from negative to positive velocity can be detected, see Figures 9-11 for respective case.

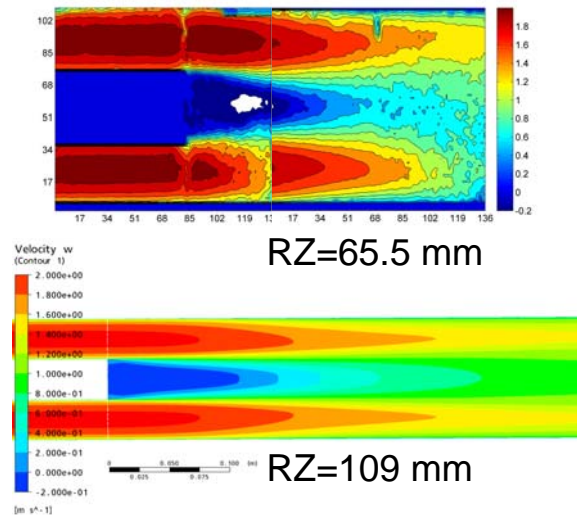


Figure 9: Equal distribution in the channels. Contour plots, PIV results (time-averaging of 6 seconds) at the top, simulation results down below.

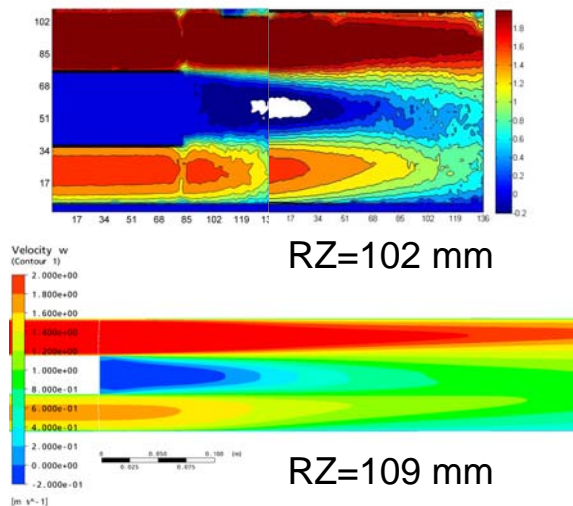


Figure 10: 60/40 distribution in the channels. Contour plots, PIV results (time-averaging of 6 seconds) at the top, simulation results down below.

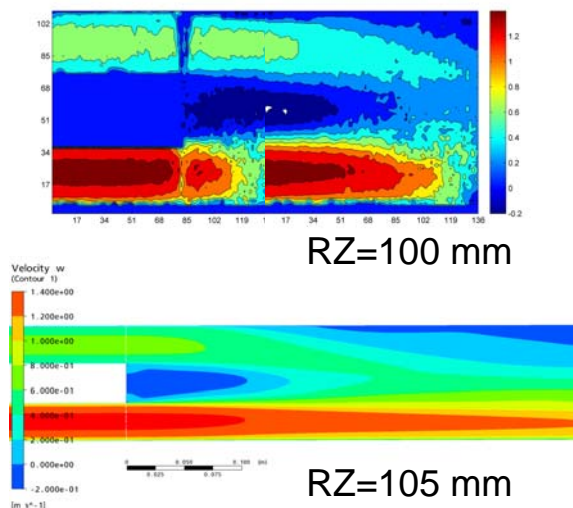


Figure 11: 70/30 distribution in the channels. Contour plots, PIV results (time-averaging of 6 seconds) at the top, simulation results down below.

Agreement between simulations and experiments are best when one of the inlet jets is dominant. The length of the recirculation zone is a clear measurement of the effect of the transient, oscillating behaviour and the way it improves the mixing and reduces the recirculation zone. A comparison of the length of the recirculation zone between experiments and simulations for the different distributions can be seen in Table 1.

Distribution		50/50	60/40	70/30
Length RZ (mm)	Experiment	65.5	102	100
	Simulation	109	109	105

Table 1: Length of the recirculation zone.

In the 50/50 case the length of the recirculation zone is about 65% longer in the simulations than in the experiments. This is because of the large amplitudes of the oscillations, a feature which is missed in steady state simulations.

CONCLUSIONS

The flow field and the recirculation zone are not affected if Re is lowered from $1 \cdot 10^5$ to $5 \cdot 10^4$. Hence there is no need for exact agreement of Re between model and reality as long as the flow is fully turbulent. Gravity does not affect the flow field pattern or the recirculation zone in a noticeable way, therefore gravity can be neglected in cold flow simulations.

The distribution of the mass flow between the two inlet channels strongly affects the overall flow field and the length of the recirculation zone. With equal distribution oscillations with large amplitudes are seen in the kiln in the experiments. The amplitude decreases when one of the inlet jets becomes dominant and the smallest oscillations can be seen in the 70/30 case. The dominant jet attracts the other one and stabilises the flow field. Because of this the steady state simulations show better agreement with the time-averaged 60/40 and 70/30 measurements.

In general, the steady state simulations show good agreement with the time-averaged results from the validation experiments. The main features of the flow field are captured and the simulation time is short compared to a transient simulation on the same mesh. Precautions should though be taken when analysing the extension of the recirculation zone. The steady state simulation does not show the transient behaviour of the flow which affects the size of the recirculation zone considerably.

Future work includes further analysis and comparison between the simulations and the experiments. Much information was retrieved in the experiments which can be used for further validation. In an ongoing work transient simulations are carried out in order to compare time-resolved simulations and experiments. Performing further PIV measurements in other planes will also be done in the future. This in order to experimentally visualise the secondary flow (flow in the transverse plane, perpendicular to the mean axial flow) arising in the half circular channels. Changing the inlet channels angles to see how the incoming flow angle affects the flow field is another possible future project.

ACKNOWLEDGEMENTS

This work was carried out within the framework of the Faste Laboratory, a VINNOVA Excellence centre. The authors also acknowledge discussions with Prof. Graham Nathan from the University of Adelaide and with LKAB.

REFERENCES

- ANSYS CFX-SOLVER THEORY GUIDE (2006), Elsevier Academic Press.
- BUNDERSON, N.E. and SMITH B.L., (2005), "Passive mixing control of plane parallel jets", *Experiments in Fluids*, **39**, 66-74.

CASEY, M. and WINTERGERSTE, T., (2000), "Best Practice Guidelines", *Special Interest Group on "Quality and Trust in Industrial CFD"*, 1 ed.

DEAN, R.B. and BRADSHAW, P., (1976), "Measurements of interacting turbulent shear layers in a duct", *J. of Fluid Mechanics*, **78(4)**, 641 – 676.

MULLINGER, P. and JENKINS, B., (2008), "Industrial and process furnaces: principles, design and operation", *Butterworth-Heinemann*, 1 ed.

SCHNEIDER, G. M. and NATHAN, G. J. and O'DOHERTY, T., (2004), "Implications on flame stabilization in a precessing jet flame from near field velocity measurements", *Proceedings of the Institution of Mechanical Engineers*, **218**, 677-687.

YIN, Z-Q. and ZHANG, H-J. and LIN, J-Z., (2007), "Experimental study on the flow field characteristics in the mixing region of twin jets", *Journal of Hydrodynamics*, Ser. B, **19(3)**, 309-313.